

2 Close-by showers separation within SDHCAL 3 prototype detector using ArborPFA

R. Été^{a*}

^a *Université de Lyon, Université Lyon 1, CNRS/IN2P3, IPNL, 4 Rue E. Fermi, 69622
Villeurbanne Cedex, France*

4 *E-mail:* rete@ipnl.in2p3.fr

ABSTRACT:

A new reconstruction algorithm called ArborPFA is developed to separate close-by hadronic showers in the SDHCAL prototype. This intends to demonstrate the capability of high granularity hadronic calorimeters such as the SDHCAL to apply efficiently the Particle Flow Algorithms in the future ILC experiments. The reconstruction algorithm we present here uses the tree structure features of the hadronic showers, that high granular calorimeters reveal, to associate clusters belonging to each hadronic shower and to reduce the confusion between two close-by showers. The results of these studies indicate a good single particle efficiency and powerful separation down to 5 cm of separation distance.

*Corresponding author.

7 **Contents**

8	1. Introduction	2
9	2. The SDHCAL prototype	3
10	3. The Arbor particle flow algorithm	4
11	3.1 Principle	4
12	3.2 Pre-clustering phase	5
13	3.3 The main clustering phase - Connectors and trees	6
14	3.4 Association algorithms	8
15	4. Single particle study	12
16	4.1 Setup	12
17	4.2 Single particle analysis	12
18	5. Separation of two close-by hadronic showers	14
19	5.1 Overlay procedure and setup	14
20	5.2 Overlaid particles analysis	15
21	6. Summary	18
22	A. ArborPFA algorithm parameters	20
23	B. SDHCAL data	26

25 Keywords: Particle flow; Calorimetry; ILC; SDHCAL

1. Introduction

To study the Higgs boson properties and to extend the discovery of new particles beyond the scope of LHC, a linear $e^+ e^-$ collider such as the ILC is proposed. An important requirement of such a machine is to provide a good jet energy resolution ($\Delta E/E \sim 3-4\%$) in order to distinguish between Z and W^\pm bosons as well as to study the Higgs boson properties. To achieve this, both good energy resolution and fine transverse segmentation should be provided by the *electromagnetic calorimeter* (ECAL) and the *hadronic calorimeter* (HCAL).

Different calorimeters are currently under study by the CALICE collaboration to fulfill these requirements. In this framework, a *semi digital hadronic calorimeter* prototype (SDHCAL) was built [1] and successfully tested at the CERN H6 test beam lines of the SPS (CERN) in 2012. With a transverse readout segmentation of 1 cm^2 , 48 sampling layers and a good energy resolution [1], this calorimeter perfectly fits the ILC needs.

The Particle Flow concept has been proposed to achieve the ILC benchmarks [2]. This algorithm aims to individually reconstruct particles using the most appropriate sub-detector for the energy and momentum measurement. An implementation of the particle flow algorithm called PandoraPFA has been developed [4] and successfully applied in ILD physics performance studies and to close-by hadronic showers separation using AHCAL beam test data

In this paper, we present an other approach of the particle flow : the ArborPFA approach. The algorithm has been designed for high granularity calorimeters and tested on SDHCAL test beam data. We propose to evaluate the performance of the algorithm on single pion events and then to study the ability of the algorithm to separate two overlaid pion showers with different separation distances and different energies.

48 2. The SDHCAL prototype

49 The SDHCAL prototype is a sampling calorimeter which consists of 48 layers (up to 50 layers)
 50 alternating a 20 mm steel absorber slice and a 6 mm gas resistive plate chamber (GRPC) slice with
 51 their embedded electronics. The gas gap between the two electrodes of the GRPC is 1.2 mm. 9216
 52 pads (96 x 96) of 1cm² compose the readout of each chamber, leading to a total number of 442368
 53 channels. A complete description of the calorimeter setup and its features can be found in [1].

54 The test beam data used in this paper have been taken at the CERN H6 beam line in 2012. The
 55 pion event selection is also performed according to the selection presented in [1].

56 The reconstructed energy of a single particle is computed as follows :

$$E_{rec} = \alpha(N_{hit}) \cdot N_1 + \beta(N_{hit}) \cdot N_2 + \gamma(N_{hit}) \cdot N_3 \quad (2.1)$$

57 where α , β and γ are quadratic functions of the number of hits N_{hit} and N_1 , N_2 and N_3 are the
 58 number hits of threshold 1, 2 and 3, where $N_{hit} = N_1 + N_2 + N_3$. The nine parameters of these
 59 functions are extracted from a χ^2 minimization :

$$\chi^2 = \sum_{evt} \frac{(E_{beam} - E_{rec})^2}{E_{beam}} \quad (2.2)$$

60 This minimization was performed over all the hadronic events in the energy range [10, 80] GeV by
 61 step of 10 GeV. The linearity and energy resolution will be shown in the section 4 dedicated to the
 62 single particle study.

3. The Arbor particle flow algorithm

3.1 Principle

The Arbor approach has been developed by the ALEPH collaboration and adapted [6] for ILD detector design recently. It is based on the idea that the hadronic shower development follows a tree topology.

Figure 1 shows the shower development after a proton interaction (left) for which we can see the multiple components of the shower : charged particles, neutral particles, electromagnetic and hadronic parts. The same figure shows on the right a sampling calorimeter view of a shower interaction as seen in a high granular calorimeter. The black arrows drawn on this view suggest clearly the tree topology development of the shower.

With such an approach, the shower reconstruction follows a principle close to the underlying physics and can be useful for studying the shower structure.

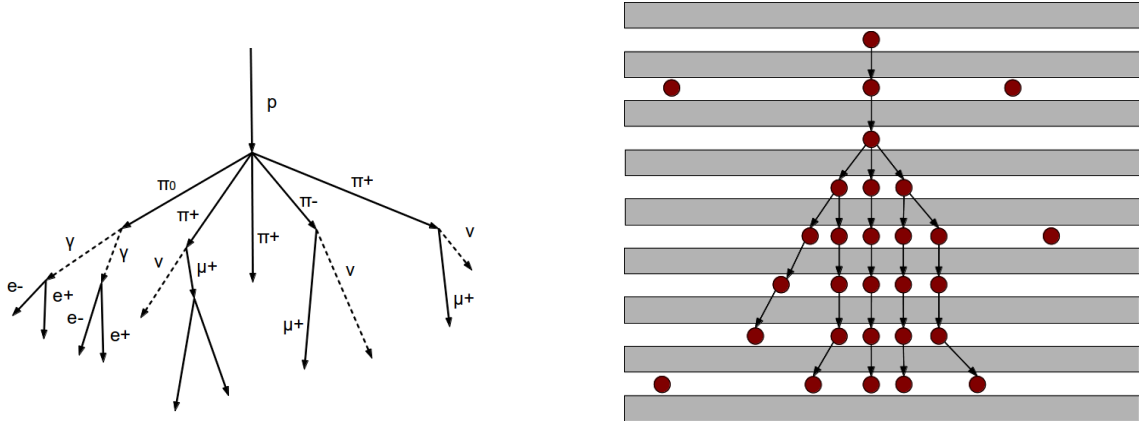


Figure 1: Left : schematic view of an induced proton shower. Right : schematic view of a reconstructed shower in a calorimeter with calorimeter hits (red)

The algorithm we present here is implemented using the PandoraSDK API as a toolkit for generic PFA development [5]. The API is used in a Marlin [3] c++ processor as part of the reconstruction chain in ILCSoft [7]. It produces only a ROOT [8] file containing the variable needed for the analysis described in this document.

Before describing the algorithm contents in detail, few definitions specific to ArborPFA need to be introduced :

Object An *object* is a calorimeter hit or a group of contiguous calorimeter hits within a layer that serves as a vertex for the ArborPFA algorithm. This was introduced for two reasons i) to provide a generalization of connections between *objects* without making any assumptions of what is contained in an *object*, ii) to overcome the track multiplicity¹ in gaseous based calorimeters such as SDHCAL [1].

¹More than one pad could be fired when a particle crosses the gas gap.

86 **Flow direction** The flow direction is of two kinds : forward direction which is from upstream to
 87 downstream of the beam direction and backward direction for the opposite.

88 **Connector** A connector is a link between two *objects*. It has a weight and a direction.

89 **Connector depth** The connector depth is defined as the number of intermediary connectors link-
 90 ing two different objects.

91 **Tree** A tree is a set of *objects* connected in a tree topology which means that for each object there
 92 is only one backward connector. An *object* without backward connector is called a seed and an
 93 *object* without a forward connector is called a leaf.

94 **Cluster** A cluster is a set of trees.

95 **Particle flow object (PFO)** A particle flow object is a set of clusters and tracks ², which corre-
 96 sponds to a reconstructed particle.

97

98 Note that in the following algorithm descriptions, some parameters are labelled by a name or a
 99 symbol and their values are given in Appendix A.

100 3.2 Pre-clustering phase

101 Before building trees, we need to create objects to connect with each others.

102 **Object creation** When a particle goes through the
 103 detector, several pads can be fired in a single layer and
 104 leads to a multiplicity greater than 1. To overcome the
 105 problem, intra-layer group of hits are assembled using
 106 the nearest neighbour clustering algorithm. For each
 107 group of hits, if its size is greater than 4, the group
 108 is split up and each of these hits becomes an object.
 109 This happens generally in the main part of a shower.
 110 Otherwise, an object is created and thus contains from
 111 1 up to 4 calorimeter hits. This is the case for a mip or
 112 an isolated group of hits. Figure 2 shows the output of
 113 this algorithm with encircled hits forming objects.

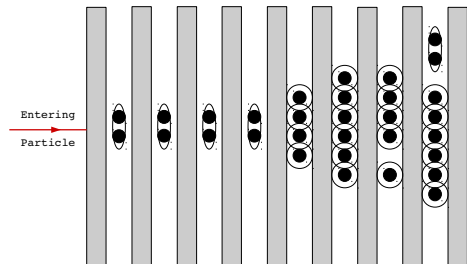


Figure 2: Schematic view of the object creation output. Small groups of contiguous calorimeter hits are grouped together (encircled).

114 **Track segment candidate tagging** In order to retrieve correctly the primary track in the calorime-
 115 ter, track segment candidates *objects* are identified and tagged for a future treatment. For each
 116 object, we count the number of neighbouring objects within the same layer at a maximum distance
 117 of Δ_{mip} . If this number doesn't exceed $N_{obj, cut}$, it is tagged as a track segment candidate object.

²By track we mean a reconstructed track in a tracking detector like a TPC

3.3 The main clustering phase - Connectors and trees

The main clustering algorithm consists in an iterative procedure using dedicated algorithms in order to create and remove connectors (connector loop). At the end of this step, all the objects are arranged in a tree structure which means that each object has 0 or 1 connector in the backward direction and 0 or many in the forward one.

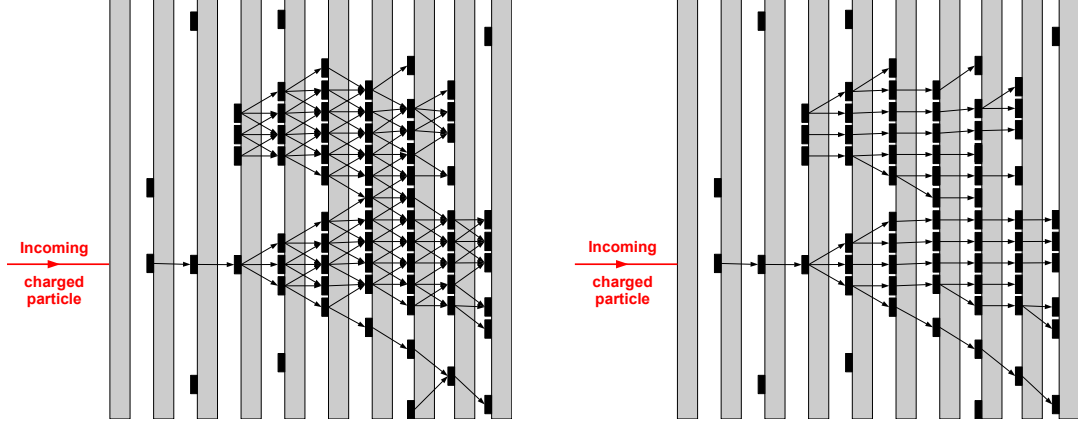


Figure 3: Schematic view of a neutral and a charged pion showers after the first connector seeding algorithm (left) and cleaning algorithm (right)

In the current implementation, the connector loop contains the following algorithms :

Primary track connection This algorithm aims to create connections between objects belonging to the primary track of charged particles in the calorimeter. It consists mainly in creating a sub-list of objects that are candidates for the primary tracks by using the objects tagged as track segment candidates and the tracks extrapolation on the front of the calorimeter. Once this list is built, the "*connector seeding 1*" algorithm and the "*connector cleaning 1*" algorithm are run on the sub list only.

Connector seeding 1 In this sub-part, we start by creating connections in the neighbourhood of each object. For each object, we look for other objects in the N_{layers} next layers with a maximum distance Δ_{max} and we create a connection between them. As an example, Figure 3 illustrates the output of this algorithm.

Connector cleaning 1 Once connectors are seeded, we need to build a tree structure by keeping only one connector in the backward direction for each object. We define the reference direction of an object as :

$$\vec{C}_{ref} = w_{bck} \cdot \sum_{\sigma} \sum_b \vec{c}_{b,\sigma} - w_{fwd} \cdot \sum_{\delta} \sum_f \vec{c}_{f,\delta} \quad (3.1)$$

where :

- w_{bck} (w_{fwd}) is the global weight assigned to backward (forward) connectors

- $\vec{c}_{b,\sigma}$ ($\vec{c}_{f,\delta}$) is the direction of a backward (forward) connector at the connector depth σ (δ) from the considered object

The depth parameter σ has been fixed to 1 in all algorithms. The reference direction is a vector that goes in the backward direction and indicates the most probable direction for a unique backward connection. Then we need to assign which backward connector should be kept for the tree building. Thus, for each backward connector of an object, we define the κ order parameter as :

$$\kappa = \left(\frac{\theta}{\pi}\right)^{p_\theta} \cdot \left(\frac{\Delta}{\Delta_{max}}\right)^{p_\Delta} \quad (3.2)$$

where :

- θ is the angle between a backward connector and the reference direction of the considered object,
- Δ is the distance between a pointed backward object and the considered object,
- p_θ (resp. p_Δ) is a power parameter for the normalized angle (resp. the normalized distance)

The κ parameter quantifies the alignment with the reference direction within the range $[0,1]$. Smaller is this parameter, higher the alignment will be. Thus, the power parameters p_θ and p_Δ are to be tuned depending on which variable we want to emphasize.

The chosen backward connector for the tree building will be the one with the smallest κ parameter; all the others are removed from the list. The removal of connectors is done at the end of the algorithm so that all connectors contribute to the evaluation of the reference direction.

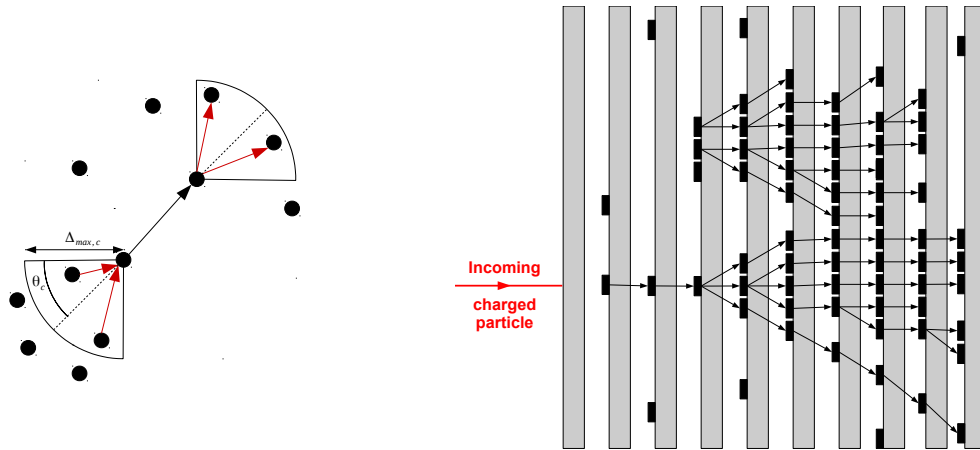


Figure 4: Left : Schematic view of the connector alignment procedure. In black, a considered connector and in red possible new connectors in backward and forward directions. Right : a neutral and a charged pion showers after the second connector cleaning algorithm

156 **Connector seeding 2** This second step of connector seeding starts from the tree structure ob-
 157 tained after the first connector cleaning algorithm. The goal of this second step is to create an
 158 alignment of connectors within the shower. For each connector, more forward connectors are cre-
 159 ated from the forward object of this connector by looking in a cone of half-angle θ_c and a maximum
 160 distance of $\Delta_{max,c}$. In the same way, more backward connectors are created from the backward ob-
 161 ject of this connector. A schematic view of this step is shown on figure 4.

162 **Connector cleaning 2** Here, we need again to clean-up the backward connector list to end up
 163 with only one connector. This last algorithm is similar to the first connector cleaning except that
 164 the cleaning is done layer per layer starting from the downstream layers with a depth parameter
 165 δ strictly higher than one. For a given connector, this accentuates the alignment with the forward
 166 ones. We end up then with a tree structure again.

167 **Tree building** This step is straight-forward. Seed objects are identified and trees are built by
 168 following the forward connected objects recursively. At this step, clusters are built each containing
 169 a single tree. The following algorithms will associate some of the trees with others.

170 3.4 Association algorithms

171 **Energy driven track cluster association** The track to cluster association is performed using two
 172 different pieces of information, the energy/momentum of the cluster/track and the cluster topology.
 173 We first look at the track projection at the calorimeter front face. Two different cases may happen :

- 174 • the particle has interacted before the calorimeter or in the first layer. In this case, many
 175 seed objects are found in the N_{layer} first layers at a maximum distance of $\Delta_{track-cluster_1}$ of the
 176 track projection. Seed objects are then sorted by their distance to the track projection. The
 177 clusters associated to their seeds are then associated to the track progressively starting from
 178 the closest one until the difference between the track momentum and the total cluster energy
 179 is minimized. The clusters are then merged since they belong to the same cluster structure.
- 180 • the particle produced a track segment at least in the N_{layer} first layers and a seed objects are
 181 found within a distance $\Delta_{(track-cluster)_1}$ to the track projection. Since only a cluster starting
 182 with a track segment has to be associated, an additional distance cut $\Delta_{(track-cluster)_2}$ between
 183 seed objects and the track projection is applied. This decreases the confusion for a small
 184 separation distance between close-by particles. The same track-to-cluster association and
 185 cluster merging is then performed as above.

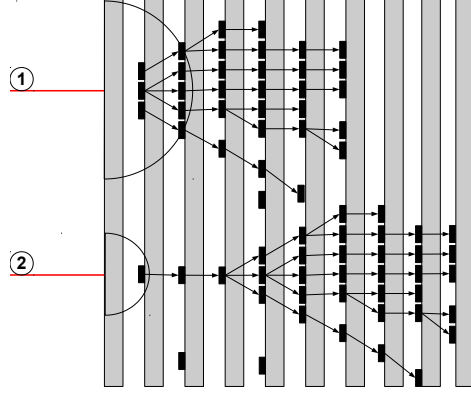


Figure 5: Schematic view of the energy driven track cluster algorithm.

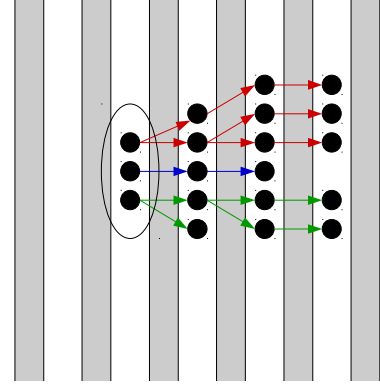


Figure 6: Schematic view of the neutral tree merging algorithm.

Figure 5 shows a schematic view of the two different scenarios. The first one corresponds to the case where an early interaction is found and the second one where a primary track segment of a cluster is found.

Neutral tree merging This algorithm is designed for neutral particle interactions for which the first interacting layer contains few seeds. Figure 6 shows a configuration where many trees have been built (with three colours) for one neutral particle interaction. We can see that the seeds in the first interacting layer belongs to the same cluster. We group all the tree seeds within the same layer and at maximum distance of Δ_{seed} . Then all of these trees are merged in the cluster.

Pointing cluster association This step aims at associating neutral fragments to other fragments which may be charged or neutral parent clusters. We start by identifying the clusters that have at least $N_{objects}$ objects in at least N_{layer} contiguous layers. The selected cluster could be either a parent or a daughter cluster. Then we proceed as follows :

1. A linear 3D straight line fit is performed over the position of all the hits of each cluster. This defines the direction of each cluster.
2. The clusters are sorted by their most downstream layers (downstream hit in the cluster) l_{inner} .
3. Starting from the most downstream cluster i , we look for a parent cluster j for which $l_{inner,i} > l_{inner,j}$.
4. Among these candidate parent clusters, we look for those for which $d_{proj} < d_{proj,cut}$ & $\theta_{i,j} < \theta_{i,j,cut}$ where :
 - d_{proj} is the distance between the candidate daughter cluster direction and the candidate parent cluster barycentre (line-to-point distance)
 - $\theta_{i,j}$ is the angle between the direction of the two clusters
and we choose the cluster for which d_{proj} is minimum.
5. Among this same list of candidate parent clusters, we look for those satisfying the condition $d_{cross} < d_{cross,cut}$ & $d_{closest} < d_{closest,cut}$ where :
 - d_{cross} is the distance at closest approach (d.c.a) between the two cluster directions

- $d_{closest,i,j}$ is the closest distance between an object of the parent cluster and the point where the daughter cluster direction crosses the parent one (distance at closest approach)

and we choose the cluster for which d_{cross} is minimal.

6. We choose the best candidate parent cluster among the two previous methods above. Many cases may happen i) no parent cluster is found, then no parent cluster is assigned to this daughter cluster, ii) one of the two methods has found a parent cluster or the two methods provide the same parent, then we assign it to the daughter cluster, iii) the two methods have found a parent cluster but there are not the same one. In this case the closest candidate parent cluster among the two in terms of barycentre distance is assigned to the daughter cluster.

7. If no parent cluster has been found for the cluster i , stop processing this cluster, else :

8. If the parent cluster has no associated track, merge the two clusters, else :

9. We define the variable Ψ as :

$$\Psi = \left| \frac{p - E_{tot}}{f_{res} \cdot \sigma_E \cdot p} \right| \quad (3.3)$$

where :

- p is the track momentum of the parent cluster
- E_{tot} is the total energy estimated from the combined hit list of the parent and daughter clusters
- σ_E is the energy resolution at the track momentum p
- f_{res} ³ is an energy resolution factor

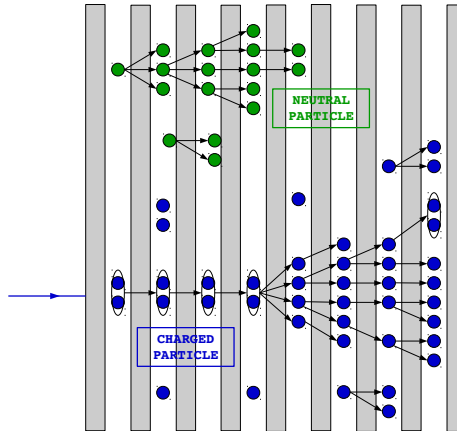


Figure 7: Schematic view of the final ArborPFA output

³The parameter f_{res} is used to reduce or enlarge the accepted range of the difference $p - E_{tot}$. A higher value of this parameter will accept a merging with a higher difference $p - E_{tot}$.

232 We check then that the Ψ^2 defined for the parent and daughter clusters is less than Ψ_{cut}^2 and
233 if the difference between p and E_{tot} after the cluster merging (parent + daughter clusters)
234 decreases. The two clusters are merged if the previous conditions are satisfied.

235 **Small neutral fragment merging** At this stage, the main part of the shower of each particles has
236 been identified. Only isolated objects and small tree structures that surround the showers are not
237 associated. First, these small structures are identified if their size is less than N_{cut} objects. Then for
238 all showers and small structures, the centroid (barycentre) is computed and each small structure is
239 merged in the shower that has the smallest distance between centroids.

240 **Particle flow object creation** Particle flow objects are built from the produced clusters after all
241 the steps described above (Figure 7). Charged PFOs are built from clusters that have an associated
242 track, while other clusters are considered as neutral PFOs.

243 4. Single particle study

244 4.1 Setup

245 To study the single particle performance, we use
 246 the SDHCAL charged pion data taken at CERN
 247 on the H6 line of SPS in 2012. The list of runs for
 248 the different energies can be found in Appendix
 249 16. In order to select only pions, an event selec-
 250 tion is performed as described in [1].

251 To emulate correctly a charged pion for the
 252 reconstruction program, a fake-track is created in
 253 front of the calorimeter. A global barycentre of all
 254 hit positions in the transverse plan is calculated.
 255 A new barycentre is then calculated using the 4
 256 first layers only and within a region of 8x8 cells
 257 around the global barycentre in the x and y direc-
 258 tion. This defines the shower entering point in the
 259 first layer. From the entering point of the shower,
 260 a straight track is created with a momentum equal to that of beams.

261 The calorimeter hits and the created track are then loaded in the PandoraSDK toolkit [5] within
 262 a single hcal endcap geometry (without the beam pipe and the BeamCal) and processed by the
 263 ArborPFA algorithms. An event display after loading the inputs in the framework is shown on
 264 figure 8.

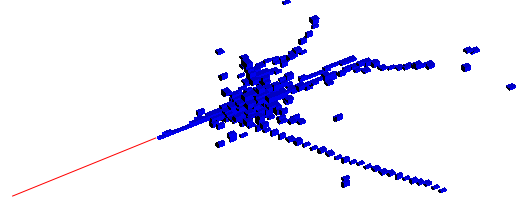


Figure 8: Event display of a 50 GeV pion shower in the SDHCAL detector as loaded in the reconstruction framework

265 4.2 Single particle analysis

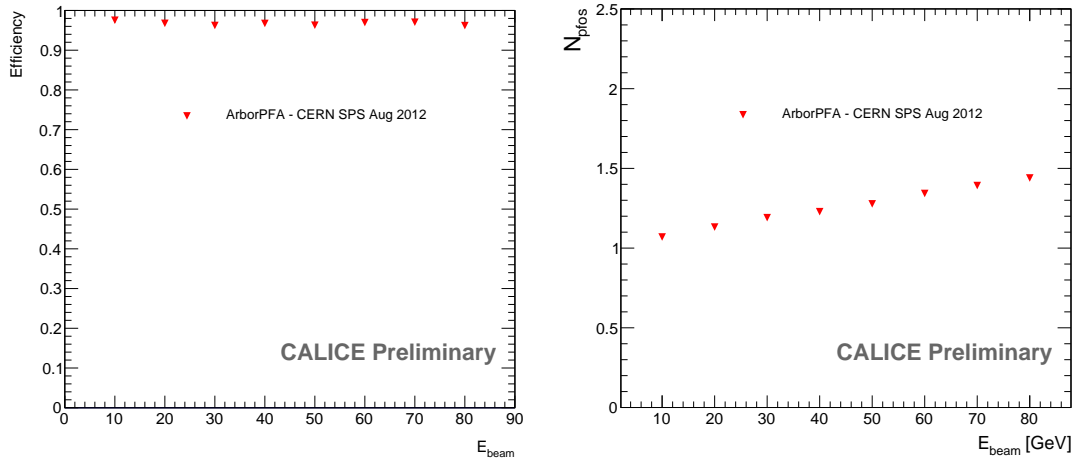


Figure 9: Efficiency of the number of recovered hits (left) and the mean number of reconstructed particles (right) after ArborPFA reconstruction on single pion shower events with the SDHCAL prototype

266 We define the efficiency of the single particle reconstruction ε_s as the number of hits recovered
 267 by the ArborPFA program and correctly attached to track in front of the calorimeter. Figure 9 shows
 268 the mean efficiency of the single particle reconstruction (left) and the mean number of reconstructed
 269 particles (right) as a function of the beam energy after applying the ArborPFA. It shows a constant
 270 efficiency with more than 95% over the whole beam energy range. But since the number of hits
 271 increases with the energy, the number of missed hits in the reconstructed charged particle increases
 272 as well. Consequently, the number of reconstructed particles shows an increase which is directly
 273 due to the shower splitting. This number grows up to 1.45 particles at 80 GeV but has finally
 274 a small impact on the reconstructed energy and energy resolution because the small additional
 275 clusters represent a small amount of energy. Indeed, figure 10 shows the reconstructed energy and
 276 energy resolution of a single charged pion before and after running the ArborPFA program.

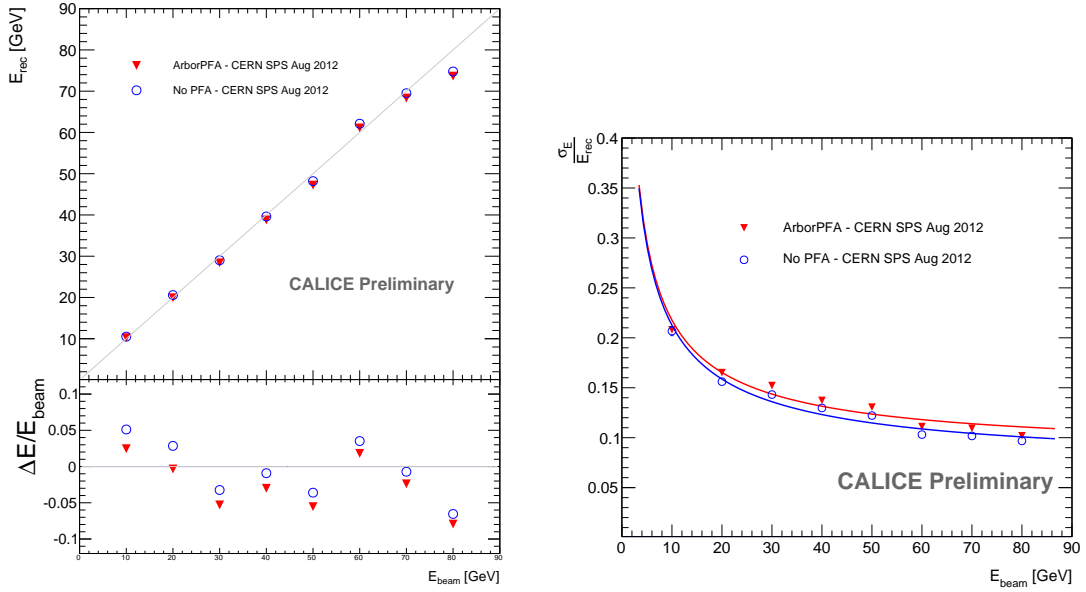


Figure 10: Reconstructed energy (left) and energy resolution (right) before (blue) and after (red) ArborPFA reconstruction on single pion shower event with the SDHCAL prototype

277 The linearity is shown below the reconstructed energy and is defined as :

$$\Delta E/E_{beam} = (E_{rec} - E_{beam})/E_{beam} \quad (4.1)$$

278 These energy points are extracted using two fits of the energy distributions i) a gaussian dis-
 279 tribution fit over the full reconstructed distribution is first performed. The mean $\mu_{E,first}$ and the
 280 width $\sigma_{E,first}$ are extracted and ii) a second gaussian fit is then performed over the range $[\mu_{E,first} -$
 281 $1.5 \cdot \sigma_{E,first} ; \mu_{E,first} + 1.5 \cdot \sigma_{E,first}]$. From the latter, we extract the final values of the reconstructed
 282 energy and energy resolution defined as the mean μ_E and the width σ_E respectively of the gaus-
 283 sian fit (same procedure applied in [1]). The efficiency plot has shown that some hits are missing
 284 after reconstruction so it is expected to have a small energy decrease in the reconstructed energy.
 285 Nevertheless, the linearity is still within 5% as before applying the reconstruction.

5. Separation of two close-by hadronic showers

The ability of a particle flow algorithm to disentangle close-by showers is a key point for the reconstruction in detectors such as ILD of the ILC. To study the confusion between neutral and charged hadrons and the ability of the ArborPFA algorithm to disentangle them, we use again the same test beam data of the SDHCAL prototype. Two different pion showers are first overlaid in the same event and the ArborPFA algorithm is run on the overlaid event with the same parameters as for the single particle study. An analysis of the separation is then performed in order to extract the performance of the algorithm.

5.1 Overlay procedure and setup

In order to study the separation of close-by hadronic showers, two events from test beam data are overlaid in one event. We have chosen to overlay 10 GeV pions and pions with different energies from 10 GeV up to 50 GeV by step of 10 GeV. Different separation distances between the shower entry point from 5 cm up to 30 cm by step of 5 cm were used. The choice of this energy range is motivated by the fact that it is the typical single particle energies foreseen at the ILC within jets [2].

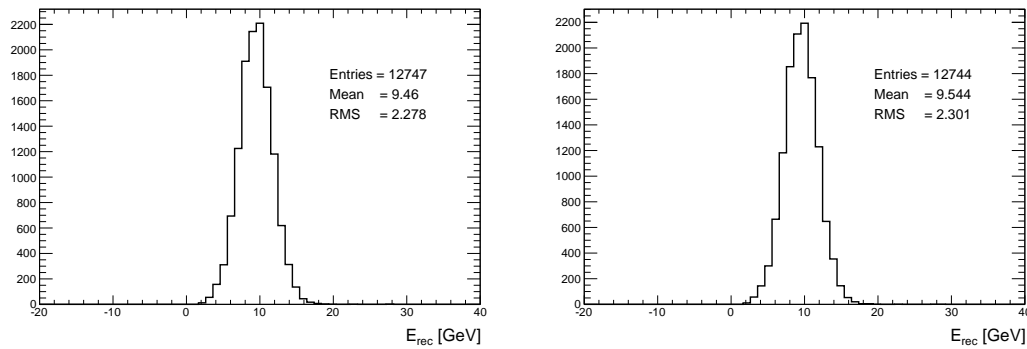


Figure 11: The reconstructed energy of the 10 GeV neutral hadron after the overlay procedure with a 50 GeV charged hadron with a separation distance of 30 cm (left) and 5 cm (right)

The overlay event algorithm is processed as follow :

1. The entering track segments of the two showers are determined as for the single particle case. This allows to identify the shower entering points and starting points.
2. For one of the two pion showers, the hits belonging to its track segments, if any, are removed from the event in order to emulate a neutral hadron shower.
3. The two showers are then centred along the X and Y axis at the center of the calorimeter. No shift is performed on the Z direction (beam line).
4. The showers are then shifted along the X axis by a distance of $-d/2$ for the neutral hadron and $+d/2$ for the charged particle.

- 310 5. The two events are then overlaid in a new one. At this step a problem may occur : while
 311 mixing the showers in the event, pair of hits may overlap in the same cell. Knowing that we
 312 are using a semi digital readout and that the information of the deposit charge in each cell
 313 is not available in the data, we need to assign a new threshold by using an approximation.
 314 The most intuitive one is to keep the highest threshold of the two hits. Figure 11 shows the
 315 reconstructed energy of the 10 GeV neutral hadron overlaid with a 50 GeV charged hadron
 316 at 30 cm distance (left) and 5 cm distance (right). The latter case is the worst one that can
 317 appears in this study given the energy points and the distances we have chosen. By comparing
 318 the two plots, we can see that the effect of this approximation on the reconstructed energy is
 319 negligible.
- 320 6. The hits are tagged with respect to our initial showers. All the hits of the neutral hadron are
 321 tagged 1 while for the charged hadron the hits are tagged 2. The overlaid hits are tagged 3 so
 322 that the information on the overlaid hits can be retrieved after reconstruction.
- 323 7. A new event is created containing the overlaid showers and the entering point of the charged
 324 particle track after shifting as shown on figure 12.

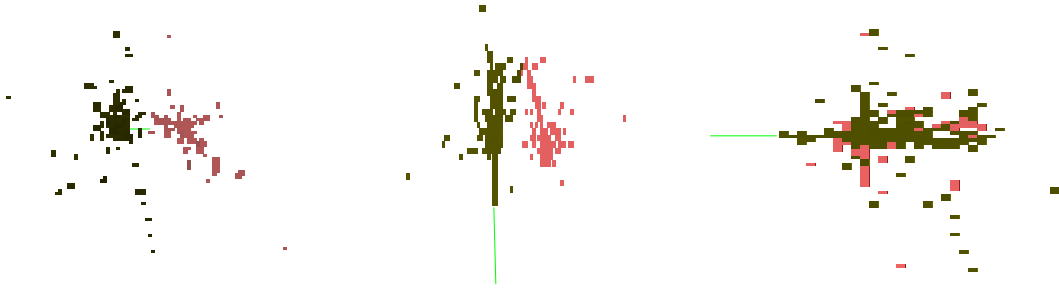


Figure 12: Event display of a 10 GeV neutral hadron overlaid with a 30 GeV charged hadron at 20 cm separation distance on three different views (XoY on left, XoZ in center and YoZ on right). Colours correspond to the reconstructed PFOs after running the ArborPFA program. The green straight line is the track generated in front of the calorimeter.

325 5.2 Overlaid particles analysis

326 Figure 13 shows the mean number of PFOs after running the ArborPFA program on a 10 GeV neu-
 327 tral hadron overlaid with a charged hadron at different energies and different separation distances
 328 between them. The behaviour at a large separation distances where the number of PFOs increases
 329 with the charged particle energy matches the behaviour of the number of PFOs in the single particle
 330 study. We can also see that the sum of the number of PFOs for the single particle is compatible
 331 with the number of PFOs for the overlay. The mean number of PFOs is stable at large separation
 332 distances but decreases for distances shorter than 10 cm from 2.1 PFOs down to 1.8 PFOs due to
 333 the showers overlap and confusions.

334 To quantify the separation, we define the efficiency and the purity related to the reconstruction
 335 of one of the two related showers as :

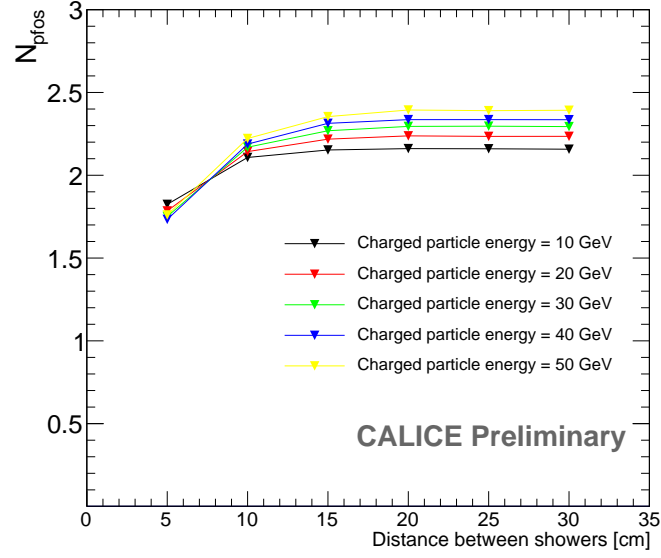


Figure 13: The mean number of PFOs after running the ArborPFA program on overlaid particles.

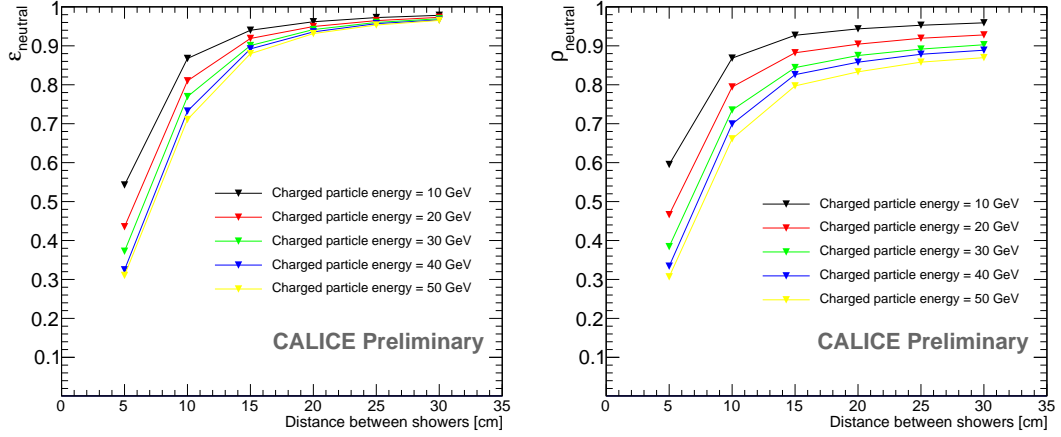


Figure 14: The efficiency (left) and purity (right) of the 10 GeV neutral hadron after separation with a charged hadron

$$\epsilon = \frac{N_{hit_{good}}}{N_{hit_{ini,tot}}} \quad (5.1)$$

$$\rho = \frac{N_{hit_{good}}}{N_{hit_{rec,tot}}} \quad (5.2)$$

336

337 with $N_{hit_{good}}$ the number of hits that initially belong to the particle and correctly assigned
 338 after reconstruction, $N_{hit_{rec,tot}}$ the total number of hits of the reconstructed shower and $N_{hit_{ini,tot}}$
 339 the total number of hits of the particle before reconstruction.

Figure 14 shows the efficiency (left) and the purity (right) of the neutral hadron for different charged particle energies and different separation distances. In the same way as for the mean number of PFOs, at small distances the two showers start to overlap and confusions appear while the reconstruction is performed. Thus, some hits of the neutral hadron are assigned to the charged one (and vice versa) and the efficiency and purity decrease. At large separation distances, the purity does not tend to 100%. This is due to the last performed algorithm (small neutral fragment algorithm) which tends to merge the small neutral cluster fragments in their closest parent cluster, without taking care of the parent cluster size or energy. Since the number of neutral fragments for a single hadron particle increases with the energy, a non-negligible part of the charged hits is assigned to the neutral hadron, leading to a decrease of its purity.

Figure 15 (on the left) shows the fraction of events where at least one neutral hadron has been reconstructed. As expected, the number of reconstructed neutral particles decreases with the separation distance. From 30 cm down to 15 cm, this fraction is stable and very closed to 100%. At 10 cm, confusions start appearing and the neutral hadron is sometimes merged in the charged one, leading to a small decrease of this fraction. At 5 cm, we can see that the fraction strongly depends on the charged particle energy and goes from 73% of reconstructed events for the 10 GeV charged particle case down to 60% for the 50 GeV charged particle case.

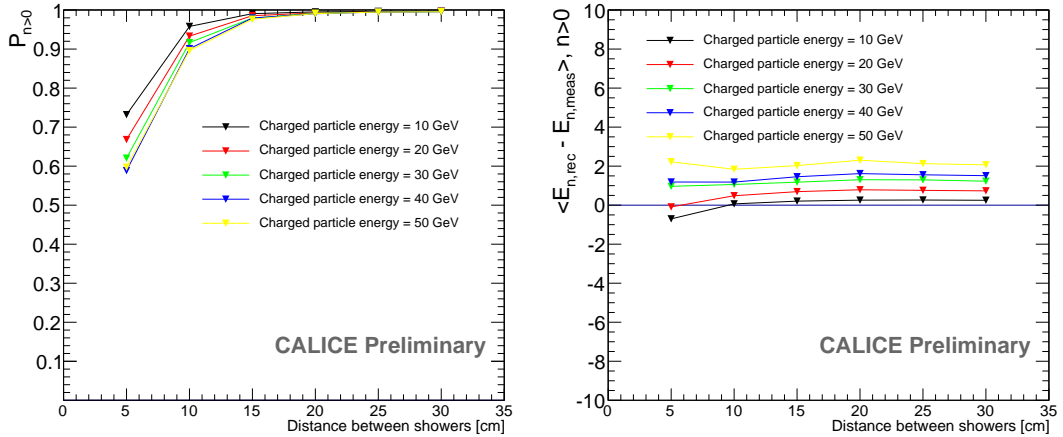


Figure 15: Left : The fraction of events where at least one neutral hadron has been reconstructed.
Right : The same variable when at least one neutral hadron has been reconstructed.

Figure 15 (on the right) shows the mean difference between the reconstructed energy and the measured energy of the neutral hadron in the case where at least one neutral hadron has been reconstructed. In the same way as for the purity, the reconstructed energy of the neutral hadron increases with the charged particle energy. This plot also shows a constant evolution of the reconstructed energy with the separation distance. This means that the reconstruction of the neutral hadron at very small distance (5 cm) has a *binary-like* behaviour, either well reconstructed or completely merged in the charged hadron.

6. Summary

The ArborPFA algorithm has been described in details with all the sub-algorithms.

A single particle study has been performed on SDHCAL test beam data taken at SPS at CERN during August and September 2012 [1]. Single pion showers have been selected and a track in front of the calorimeter has been created in order to emulate a TPC track.

The results showed a good efficiency with more than 95% of hits assigned to the reconstructed charged particle over the whole energy range. The mean number of PFOs shows an increase with the energy from 1.1 PFOs at 10GeV up to 1.4 PFOs at 80 GeV growing linearly. The reconstructed energy of the single charged hadron is close to the one applied before running the algorithm with a small decrease due to the 5% of inefficiency and thus the energy resolution increases too.

The algorithm has also been applied in order to separate close-by hadronic showers. Two different charged hadron showers with different energies from the same test beam data set have been overlaid in the same event with different separation distances. For one of the two showers the mip track inside the calorimeter has been identified and removed from the event in order to emulate a neutral hadron particle. For the other particle, a track has been generated in front of the calorimeter and pointing on the particle entry point, as for the single particle case.

The results showed a good neutral hadron efficiency and purity until 10 cm separation distance where a non negligible confusion starts to appear.

The difference between the reconstructed energy and the measured energy of the neutral hadron in the case where at least one neutral hadron has been reconstructed showed an increase with the charged hadron energy for all the separation distances due to the small neutral fragment merging algorithm. At small separation distance (5cm), the difference stays constant and shows that the neutral hadron reconstruction has a *binary-like* behaviour, either a very good reconstruction or merged in the charged hadron.

This work will be extended shortly to include the electromagnetic calorimeter as well as the other sub-detectors in the framework of the ILD detector with the aim to separate charged and neutral hadrons produced in jets to improve on the PFA performances.

References

- [1] Calice Collaboration, *First results of the CALICE SDHCAL technological prototype*, CAN-037
- [2] J. Carwardine *et al.*, *International Linear Collider Technical Design Report*. 1) Executive Summary, 2) Physics, 3) Accelerator, 4) Detectors. 12 June 2013
- [3] F. Gaede, Marlin and LCCD: Software tools for the ILC, Nucl.Instrum.Meth. A559 (2006) 177-180
- [4] M. A. Thomson, *Particle Flow Calorimetry and the PandoraPFA Algorithm*,
phys.int-det/0907.3577
- [5] J. S. Marshall, M. A. Thomson, *The Pandora Software Development Kit for Pattern Recognition*,
phys.int-det/1506.05348
- [6] M. Ruan, *Arbor, a new approach of the Particle Flow Algorithm*, Proceeding of CHEF 2013.
hep-ex/1403.4784
- [7] ILCsoft, 2012. <http://ilcsoft.desy.de/portal>
- [8] ROOT, 1995-2015, <https://root.cern.ch/drupal>

404 A. ArborPFA algorithm parameters

405 Object creation algorithm

Parameter name	value
MaxClusterSize	4
IntraLayerDistance	11 mm

- 406 • MaxClusterSize
- 407 → The maximum intra layer cluster size to build an object with. Else the object is split in
- 408 single calo hit objects

- 409 • IntraLayerDistance
- 410 → The nearest neighbour intra layer clustering maximum distance

411 Track segment candidate tagging algorithm

Parameter name	value
MaxNNeighbors	6
IntraLayerNeighbourDistance (Δ_{mip})	50 mm

- 412 • MaxNNeighbors
- 413 → The maximum number of neighbouring objects within a layer
- 414 • IntraLayerNeighbourDistance (Δ_{mip})
- 415 → The maximum distance between two neighbours in a layer used for the neighbour count-
- 416 ing

417 **Primary track connection**

Parameter name	value
ConnectionDistance	110 mm
BackwardConnectorWeight	2
ForwardConnectorWeight	3
OrderParameterAnglePower	1
OrderParameterDistancePower	5
MaxNEmptyConsecutiveLayers	3

- 418 • ConnectionDistance
 419 → The maximum connection distance used for the primary track connectors creation
- 420 • BackwardConnectorWeight
 421 → The backward connector weight assigned for the reference vector computation
- 422 • ForwardConnectorWeight
 423 → The forward connector weight assigned for the reference vector computation
- 424 • OrderParameterAnglePower
 425 → The angle power parameter of the κ parameter while cleaning connectors
- 426 • OrderParameterDistancePower
 427 → The distance power parameter of the κ parameter while cleaning connectors
- 428 • MaxNEmptyConsecutiveLayers
 429 → The maximum consecutive empty layers to take into account for the connector seeding

430 **Connector seeding 1**

Parameter name	value
ConnectionDistance	45 mm

- 431 • ConnectionDistance
 432 → The maximum connection distance used for a connector creation

433 Connector cleaning 1

Parameter name	value
BackwardConnectorWeight	2
ForwardConnectorWeight	2
OrderParameterAnglePower	1
OrderParameterDistancePower	5
ReferenceDirectionDepth	1

- 434 • BackwardConnectorWeight
- 435 → The weight of a backward connector assigned in the reference direction vector calculation.
- 436 • ForwardConnectorWeight
- 437 → The weight of a forward connector assigned in the reference direction vector calculation.
- 438 • OrderParameterAnglePower
- 439 → The θ angle power parameter used for the κ parameter computation
- 440 • OrderParameterDistancePower
- 441 → The Δ distance power parameter used for the κ parameter computation
- 442 • ReferenceDirectionDepth
- 443 → The forward connector depth used for the reference vector computation

444 Connector seeding 2

Parameter name	value
ConnectionDistance	65 mm
ConnectionAngle	0.7 rad

- 445 • ConnectionDistance
- 446 → The maximum connection distance used for a connector creation
- 447 • ConnectionAngle
- 448 → The maximum angle between two connectors

449 Connector cleaning 2

Parameter name	value
BackwardConnectorWeight	0.1
ForwardConnectorWeight	5
OrderParameterAnglePower	1
OrderParameterDistancePower	5
ReferenceDirectionDepth	2

- 450 • BackwardConnectorWeight
451 → The weight of a backward connector assigned in the reference direction vector calculation.
- 452 • ForwardConnectorWeight
453 → The weight of a forward connector assigned in the reference direction vector calculation.
- 454 • OrderParameterAnglePower
455 → The θ angle power parameter used for the κ parameter computation
- 456 • OrderParameterDistancePower
457 → The Δ distance power parameter used for the κ parameter computation
- 458 • ReferenceDirectionDepth
459 → The forward connector depth used for the reference vector computation

460 Energy driven track cluster association

Parameter name	value
TrackToClusterDistanceCut1	75 mm
TrackToClusterDistanceCut2	55 mm
FirstInteractingLayerNSeedCut	15
TrackToClusterNLayersCut	3
TrackClusterPsi2Cut	3
Psi2SigmaFactor	1.5

- 461 • TrackToClusterDistanceCut1
462 → The maximum distance between the track projection at calorimeter front face and a cluster
463 seed. This distance is used to detect an early interacting cluster.
- 464 • TrackToClusterDistanceCut2
465 → The reduced maximum distance between the track projection at calorimeter front face and
466 a cluster seed. This distance is used when no early interacting cluster has been detected.

- 467 • FirstInteractingLayerNSeedCut
468 → The cut on the number of cluster seeds found within a the distance TrackToClusterDis-
469 tanceCut1 to detect an early cluster interaction.
- 470 • TrackToClusterNLayersCut
471 → The number of inner layers to look for cluster seeds to associate.
- 472 • TrackClusterPsi2Cut
473 → The ψ^2 cut applied while associating clusters to a track.
- 474 • Psi2SigmaFactor
475 → The f_{res} factor on denominator used to compute the ψ^2 for track-to-cluster compatibility
476 (see equation 3.3)

477 Neutral tree merging

Parameter name	value
SeedSeparationMerge (Δ_{seed})	25 mm

- 478 • SeedSeparationMerge (Δ_{seed})
479 → The maximum distance between two cluster seeds within a layer to perform a cluster
480 merging

481 Pointing cluster association

Parameter name	value
MinNObjects	4
MinNLayers	4
FitToBarycentreDistanceCut	30 mm
FitToBarycentreAngleCut	$\frac{\pi}{6}$ rad
FitToFitDistanceCut	20 mm
FitDistanceApproachCut	20 mm
Chi2NSigmaFactor	1.5
Chi2AssociationCut	1

- 482 • MinNObjects
483 → The minimum number of objects within a cluster in order to to be candidate for the
484 pointing cluster association
- 485 • MinNLayers
486 → The minimum number of layers within a cluster (outermost - innermost + 1) in order to
487 be candidate for the pointing cluster association

- 488 • FitToBarycentreDistanceCut
489 → The cut applied on the distance between the daughter cluster fit and the parent cluster
490 barycentre position (point-to-line distance)
- 491 • FitToBarycentreAngleCut
492 → The cut applied on the angle between the daughter and parent cluster fits
- 493 • FitToFitDistanceCut
494 → The cut applied on the distance between the daughter and parent cluster fits (line-to-line
495 distance)
- 496 • FitDistanceApproachCut
497 → The cut applied on the closest distance between a parent cluster object and the daughter
498 cluster crossing point at the parent and daughter cluster fit closest approach.
- 499 • Chi2NSigmaFactor
500 → The N_{res} factor on denominator used to compute the χ^2 for track-to-cluster compatibility
501 (see equation 3.3) using the merged cluster (daughter + parent)
- 502 • Chi2AssociationCut
503 → The χ^2 cut applied on the merged clusters compatibility with a track when associating a
504 neutral daughter cluster with a charged parent cluster.

505 **Small neutral fragment merging**

Parameter name	value
MaximumDaughterNObject	20
LargeDistanceCut	1000 mm

- 506 • MaximumDaughterNObject
507 → The maximum number of objects to consider the cluster as a small neutral fragment to
508 merge it into a bigger parent cluster
- 509 • LargeDistanceCut
510 → The maximum distance between a small neutral fragment and a potential parent cluster

511 **B. SDHCAL data**

Energy	10 GeV	20 GeV	30 GeV	40 GeV	50 GeV	60 GeV	70 GeV	80 GeV
Run number	715693	715675	715747	715748	715751	715753	715754	715756

Figure 16: List of SDHCAL pion runs used for reconstruction

512